# Structural Analysis of Multiple Phases of Gravity Deformation in the Foz do Amazonas Basin using Seismic Interpretation and Experimental Modeling

Rodrigo Perovano (UFF/Lille I), Bruno Vendeville (Lille I), Antonio Tadeu dos Reis (UERJ), Cleverson G. Silva (UFF), Christian Gorini (Paris VI), Érika Araújo (UFF/Paris VI),



This paper was prepared for presentation during the 12th International Congress of the Brazilian Geophysical Society held in Rio de Janeiro, Brazil, August 15-18, 2011.



## Abstract

The tectonic evolution of passive margins affected by gravity-driven shale tectonics can occur through episodic events, reflecting critical stages of pore-fluid overpressure in weak lithological levels, which can lead to gravity-driven deformation (gravity gliding/spreading) of the overlying sedimentary package above multiple *décollements* levels. Based on preliminary results of seismic interpretation, experimental models were developed to replicate possible scenarios for the structural evolution of the gravitational deformation that have affected the marine sequences of the Foz do Amazonas Basin. The resulting structural setting reminds in many aspects the gravity-driven features described in the basin. An initial gravity gliding phase of a flat-layered model resulted in an upslope set of extensional faults and a downslope gravitational fold-and-thrust belt. During the second deformation phase, the gravity spreading of progradational wedges over the sliding sheet previously deformed by gravity gliding was able to promote the gradual reactivation of the compressive belt either in compression or sometimes reactivated in extension, as the shelf progrades. In all experiments, two *décollements* levels acted at some time or place supporting the gravitational deformation. The mechanical behavior of these *décollements* (silica microspheres layers) varies in time and space based on the magnitude of pore-fluid overpressure and, thus, resembles the behavior of overpressured shales.

## Introduction

Several episodes of gravitational deformation have affected the marine sequences of the Foz do Amazonas Basin, both before, and during deposition of the Amazon Fan. Gravity-driven structures are well imaged on 2-D multichannel seismic profiles and constitute a linked extensional-contractional system that comprises a distal compressional domain, an intermediate translational domain, and a proximal extensional domain (fig. 01; Reis *et al.*, 2010). All movement took place by gliding along weak lithological horizons subjected to high pore-fluid pressure probably related to upward migration of methane gas. Perovano *et al.*, (2009) and Reis *et al.* (2010) proposed simple conceptual models of a multistage structural evolution composed of two main deformation phases, in the attempt to explain both the development of paleo and "modern" fold-and-thrust belts and the distinct structural style of the NW and SW fold-and-thrust belts (figs. 02 and 03). The first stage of deformation predates the formation of the Amazon Fan, and consists of slope-parallel gravity gliding of flat layers overlying two seaward-dipping detachments (fig. 03b). The driving parameter was the basal slope. The second deformation stage took place once the Amazon Fan had formed, and consisted of gravity spreading of progradational sedimentary wedges (figs. 03c and 03d). There, the driving parameters were the bathymetric surface and the sedimentary loading, and thus the build-up of the Amazon Fan.

The main objective of the present work is to replicate the deformation phases proposed in these conceptual models by physical experimental modeling, simulating pore-fluid overpressures and integrating the main structural and stratigraphic aspects of the basin, issued by a refined age-constrained and seismic analysis. Thereby, the design and execution of models followed a planning based on the structural evolution of different generation of fold-and-thrust belts in the Foz do Amazonas Basin and, moreover, a variable structural style along the slope.

## Experimental set-up

Our experiments were carried out at the Laboratory of Evolution and Modeling of Sedimentary Basins, Université Lille I (France). During laboratory work, we designed fifteen experimental models in which compressed air, simulating methane gas in nature, was injected at the base of models composed of layers having varying permeability, hence mechanical strength (Perovano *et al*., *in preparation*). The levels located at the base of low-permeabillity layers behaved as detachment surfaces, triggering gravitational instabilities (fig. 04). The experimental apparatus allowed us to control the spatial distribution of fluid pressure. This modeling technique was originally proposed by Cobbold and Castro (1999) and recently improved by Mourgues *et al*. (2009).

Each model had 170 cm long, 60-80 cm wide, and was built between two glass side walls over the horizontal or tilted modeling table. Silica microspheres (53 - 106 μm) were used to compose the low-permeability layers, which behave as *décollement* levels during episodic fluid overpressures, due to their low permeability (10 darcy) and negligible cohesion magnitude (fig. 04). The base and interbedded fragile layers of models used coarse sands having an average granulometry of about 315 μm and 90-110 darcy of permeability (sand BE01, produced by Sifraco, France; fig. 04).

During the experiments, two main phases of gravitational deformation were simulated based on the preliminary results of seismic interpretation. A first phase of gravity gliding of flat layered models, followed by a second deformation phase involving gravity spreading of progradational coarse sand wedges above two *décollement* levels. In all the experiments, the initial gravity gliding was triggered by tilting the model (basal and surface slope - 3.5$^o$). During the second phase, part of the sedimentary wedge under pore-fluid overpressure episodes tends to translate basinward horizontal *décollements*, in response to spatial variation of lithostatic pressures between the upperslope (shelf) and downslope basin, and high angles of the wedge slope. This expanded abstract presents the results of an experiment (model 12) involving a gravity gliding phase and, subsequently, gravity spreading of five progradational sand wedges.

**Results**

**First deformation phase (gravity gliding)**

Initially, the experimental model 12 was composed of four flat-parallel layers: a lower and an upper low-permeability layers having 0,3 cm and 0,7 cm thick respectively; a interbedded fragile layer of sand of 0,5 cm thick; and an overlying fragile layer of 0,9 cm thick (fig. 04). The overpressured area had 130 cm long and 60 cm wide, and remained steady throughout the first deformation phase. According to numerical simulations, for air pressures reaching P=460 Pa, the coefficient of fluid pressure (the ratio between the pore-fluid pressure and lithostatic pressure) was maximum ($\lambda \cong 0{,}99$) at the base of the two low-permeability layers, thus it was expected the development of two *décollement* levels (fig. 04; Perovano *et al*., *in preparation*).

The gravitational deformation begins once achieved the fluid overpressure calculated to significantly reduce basal friction on the detachments, through the partial compensation of the lithostatic pressure. At this moment, an immediate slide of part of the model occurred resulting in a linked extensional-compressional system gliding on two *décollement* levels. The deformed area coincided exactly with the area affected by pore-fluid overpressure (fig. 05a). Between each episode of gliding, the accommodation space created by the tilting of the blocks on extensional faults was sequentially filled by coarse sand, in order to preserve the original lithostatic pressure and reproducing synkinematic sedimentation.

Initially, the upslope extension comprises mainly basinward and landward-dipping normal faults, stratigraphic wedges and rollover anticlines, and was limited by the western boundary of the overpressurized area (fig. 05a). Distally, thrusts faults, back-thrusts and fault-related folds were generated as a result of shortening of the section by compression (fig. 05a). During the experiment, the extensional domain migrated towards the basin, as the basinward migration of low-permeability layers blocked partially the deformation proximally (overburden touchdown; (fig. 05b). Simultaneously, many new thrusts propagated retrogressively upslope as a result of section thickening and greater resistance to fracture at the first thrust front. In the central portion of the model, a province slightly deformed, 25 cm long, connected the extensional and compressional domains (figs. 05a; b). At a late stage, a slight increase in induced overpressure ($\Delta P$ = 50 Pa) throughout the experiment was sufficient to promote deformation of areas hitherto stable. The compressive domain advanced basinward represented by a new thrust fault, limited by the eastern boundary of the overpressure area (fig. 05b). At the end of the first phase, the compressional domain was characterized mainly by eight thrust faults grouped in a wide thrust belt, covering 55% of the overpressured area (72 cm in length), which resulted from shortening of 11,5% of the section (14,5 cm in length; fig. 05b).

**Second deformation phase (gravity spreading)**

In this phase, the gravitational spreading of progradational wedges was simulated by inducing a high differential sedimentary loading between the shelf and the basin. Thus, after completing the first phase, a sedimentary wedge of coarse sand, 45 cm long and 2.8 cm thick, was built over the proximal section of the model previously deformed in extension (figs. 05c and 05a'). The shelf-break finished in a slope with 15 cm long, dipping 9$^o$ to 10$^o$. Each progradational episode of the sand wedge advanced 15 cm toward the basin, followed by basinward migration of the eastern boundary of the overpressure area, reducing its length by 15 cm (fig. 05d). Under fluid overpressure episodes, it was expected that both *décollements* levels were effective in the basin ($\lambda > 0{,}95$). In the shelf, while the lower *décollement* was fully effective ($\lambda \cong 0{,}99$), the upper *décollement* was partially limited ( $\lambda \cong 0{,}88$) by the lithostatic pressure of the cover, for a sliding pressure threshold of P=1050 Pa (fig. 04; Perovano *et al*., *in preparation*).

The gravitational spreading of the first wedge began when high air pressure was applied. The entire wedge collapsed and spread basinward in generating one extensional domain located on the shelf and upper slope, and one compressional domain located in front of the wedge's toe. The extensional domain developed over the section previously deformed in extension during the first phase (figs. 05c and 05b'). Synthetic and antithetic listric faults, grabens, stratigraphic wedges, and rollover anticlines characterize the structural domain. Most of these structures rooted on the lower detachment surface, which indicates their development linked to the level of higher efficiency. Some of the older extensional structures resulted from the gravity gliding phase were reactivated in extension, promoting the fracturing of the overlying layers (figs. 05c and 05b'). During the experiment, the graben initially formed near the shelf break, was partially inactivated at the expense of developing a prominent antithetic listric fault, which accommodated most of the extension in latter deformation stages of the first sand wedge (figs. 05d and 05b'). In the lower edges, further shortening of the section developed a couple of thrust faults, resulting in part from reactivation of previous compressional structures originated during the gliding episode (figs. 05c;d and 05c').

Afterwards, were simulated four episodes of progradation. As the gravitational system prograded, the extension took place along the ancient compressional domain, while older thrusts fronts were systematically reactivated in front of the wedge's toe (figs. 05c-g and 05a'). After each progradation, older buried paleo-thrusts were reactivated in extension. Several synthetic listric faults and grabens root on strongly thickened silica miscropheres layers, where fault-propagation folds and shear fault-bend folds were formed (fig. 05c'). Likewise, antithetic listric faults rooted on the back of folded blocks, where the upper *décollement* level had a negative slope. In the compressional domain, fault steepening and reactivation of thrust faults accommodated the additional shortening (figs. 05c-g and 05c'). Most of the thrust faults rooted on the lower detachment surface, while coupled back thrusts rooting over the upper detachment surface formed with them pop-up structures (fig. 05c'). A translational domain developed exactly over the slope and followed its progradation (figs. 05c-g). In this area, the partial reactivation of older strike-slip structures compartmentalized, even temporarily, the gravitational system (fig. 05 c-g). At the end of the experiment, the gravitational system involved the shortening of 33 cm of the section, accommodated by thrusting displacement and fault-related folding of overlying layers, which corresponds to 25,4% of the initial overpressured area (fig. 05g).

**Conclusions**

The experiments performed assisted in understanding some of the structural evolution of the gravitational system of the Foz do Amazonas Basin.

- The mechanical behavior of the silica microspheres layers varies in time and space based on the magnitude of pore-fluid overpressure and, thus, resembles the behavior of overpressured shales. For moderate pore-fluid pressures, the translation of the cover seems to have been accommodated by very thin shear zones (detachment surfaces) situated at the base of the *décollement* levels, where the coefficient of fluid pressure was maximum (fig. 04). As a result, overlying fragile layers were affected by a brittle deformation exemplified by several synthetic/antithetic listric faults, asymmetric basinward-verging thrust faults and fault-related faults (fig. 05). This resulting structural setting reminds the structural style of most of the gravity-driven features described in the Foz do Amazonas Basin (fig. 01). For high pore fluid pressures, silica microspheres layers were fluidized and moved basinward through the ductile flow and strain of the entire layer. We recognized some features, such as silica volcanoes and diapirs, which are an indication of such mechanical behaviour and attests that the pore-fluid pressure achieved locally the lithostatic stress (fig. 05). In nature, highly overpressured shales often trigger analogous features, such as mud volcanoes and shale diapirs.
- During the second deformation phase, gravity spreading of progradational wedges over a sliding sheet previously deformed by gravity gliding was able to promote the gradual reactivation of the compressive belt either in compression or sometimes reactivated in extension, as the shelf progrades (fig. 05). Similar scenarios were recognized in seismic profiles of the Foz do Amazonas Basin. Several Pleistocene listric normal faults intersect paleo-thrust-and-fold belts and detach on a Late Cretaceous detachment surface near the shelf-break. In a similar way, further shortening, induced by deposition of Amazon Fan sedimentary sequences, was accommodated by fault steepening and reactivation of some thrust fronts (figs. 02 and 03). Simultaneously, minor imbricate thrusts and other compressional features detaching on a lower *décollement* level do not propagate vertically. These structures remained buried under the upper silica microspheres layer, which acted as a roof fault with an opposite sense of shear to the basal fault, preventing an upward propagation of compressive stresses (fig. 05c'). This caused the entire sedimentary pile to thicken and sometimes to drape fold the overlying syntectonic layer by shearing stresses exerted along the two *décollement* levels (fig. 05c'). A similar behavior for the upper *décollement* level was observed in thrust-and-fold belts of the Southeastern Structural Compartment of the Foz do Amazonas Basin (fig. 02b).
- In our experiments, the spatial distribution of pore-fluid overpressure primarily controls the length of the sliding sheet. The outer limits of structural compartments coincide with the boundaries of the injection area and followed its progradation (fig. 05). These results confirm that the evolution in time and space of structural compartments of shale tectonics are potentially controlled by the spatial distribution of source rocks and, hence, gas or hydrocarbon generation rates, migration and accumulation.

**Acknowledgements**

The authors greatly acknowledge financial support and scholarships during completion of this work from the Brazilian National Research Agency (CNPq/CTPETRO), the Brazilian-French Cooperation Programme (CAPES-COFECUB) and the Brazilian National Agency of Petroleum-ANP. We also specially thank GAIA and FUGRO for the availability of additional seismic data and permission to publish main results, the Brazilian Navy for permission to use LEPLAC seismic lines, and TOTAL France for the valuable well data. We finally thank Seismic Micro-Technology Inc. for the use of educational licenses of the software *Kingdom Suite*®. This is a contribution of the research group GEOMARGEM: Geology and Oceangraphy of Passive Continental Margins (http:// www.geomargem.org).

**References**

Cobbold, P.R., & Castro, L. (1999). Fluid pressure and effective stress in sandbox models. Tectonophysics, 301, 1–19.

Mourgues, R., Lecomte, E., Vendeville, B. & S. Raillard (2009). An experimental investigation of gravity-driven shale tectonics in progradational delta, *Tectonophysics,* 474, 643-656.

Perovano, R., Reis, A.T., Silva, C.G., Vendeville, B., Araújo, E.F.S. & Gorini, C. (2009). O processo de colapso gravitacional e a estruturação da seção marinha da bacia da Foz do Amazonas- Margem equatorial brasileira. Revista Brasileira de Geofísica (Impresso), v. 27, p. 459-484, 2009.

Perovano, R., Vendeville, B., Reis, A.T., Silva, C.G.; Gorini, C. & Araújo, E.F.S.; (*in preparation*). Physical experimental models simulating main phases of gravity tectonic deformation driven by overpressured levels in the Foz do Amazonas basin. To be submitted to Journal of Structural Geology.

Reis, A.T., Perovano, R., Silva, C.G., Vendeville, B.C., Araújo, E.F.S., Gorini, C. & Oliveira, V. (2010). Two-scale gravitational collapse in the Amazon Fan: a coupled system of gravity tectonics and mass-transport processes. Journal of the Geological Society (London), v. 167, p. 593-604.

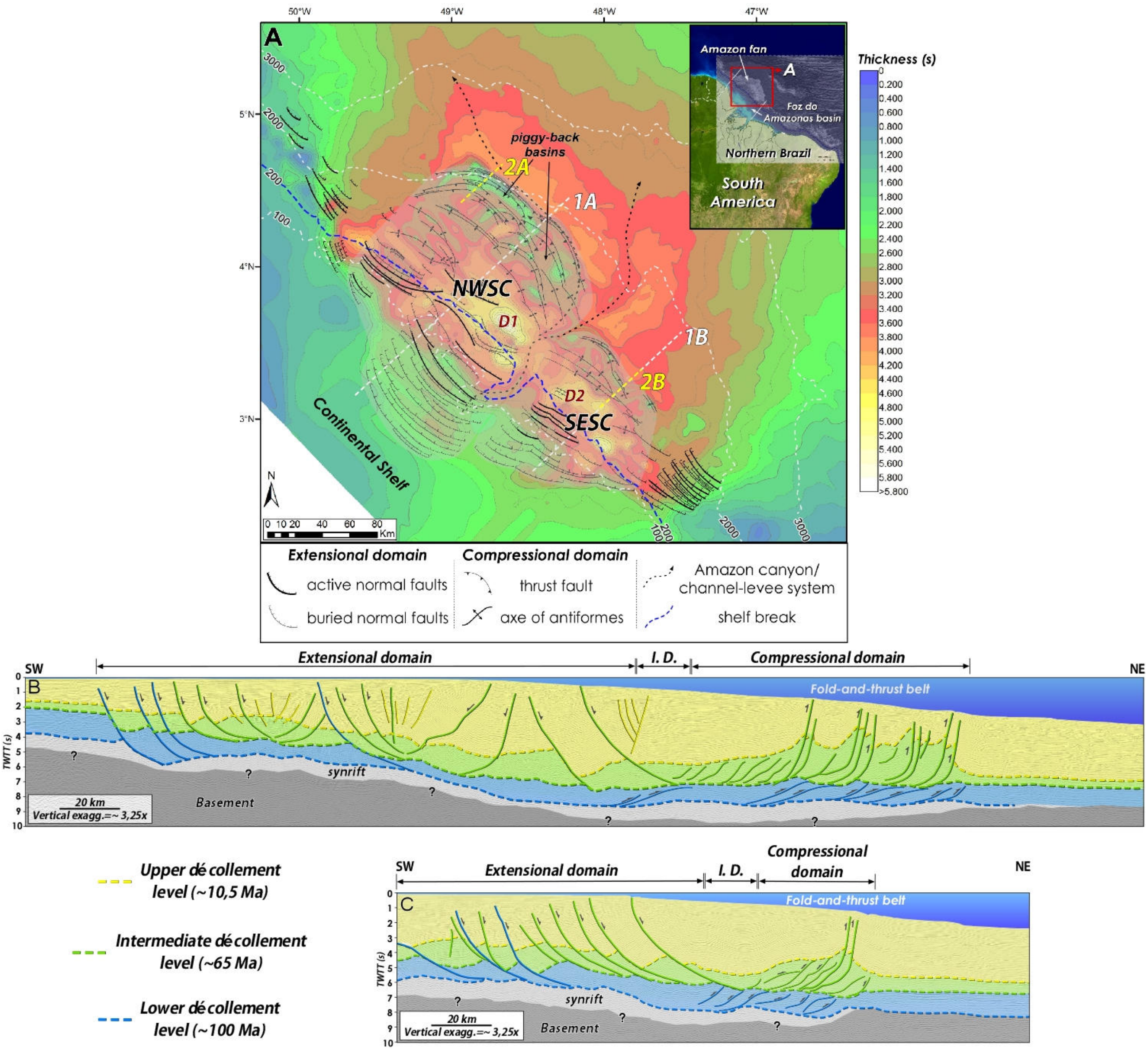


Figure 01 - (a) Integrated map of structural system of the basin's gravity tectonics with the sediment isopach data of the Amazon fan sequences (time depth to the upper *décollement* level). The Northwestern Structural Compartment (NWSC) and the Southeastern Structural Compartment (SESC) are highlighted in gray. Margin's main depocenters for the time interval considered are represented as D1 and D2. Numbers refers to figures in this paper. Bathymetric data are from a compilation made by the Brazilian Navy (Reis *et al*., 2010). Interpreted dip seismic profiles illustrating the linked extensional-compressional system gliding over multiples *décollement* levels across the (b) the NW and (c) the SE Structural Compartments of the Foz do Amazonas Basin (Reis *et al*., 2010).

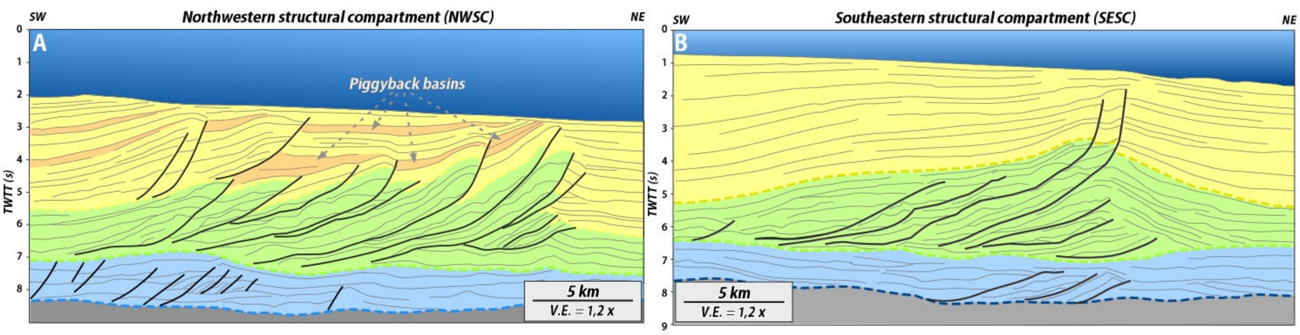


Figure 02 - Extracts of seismic lines across the compressional domain of both, (a) NW and (b) SE, structural compartments showing different structural styles and complexity of fold-and-thrust belts that stand out and affect the seafloor morphology along the upper slope. Piggy-back basins are highlighted in red (Perovano *et al*., *in preparation*).

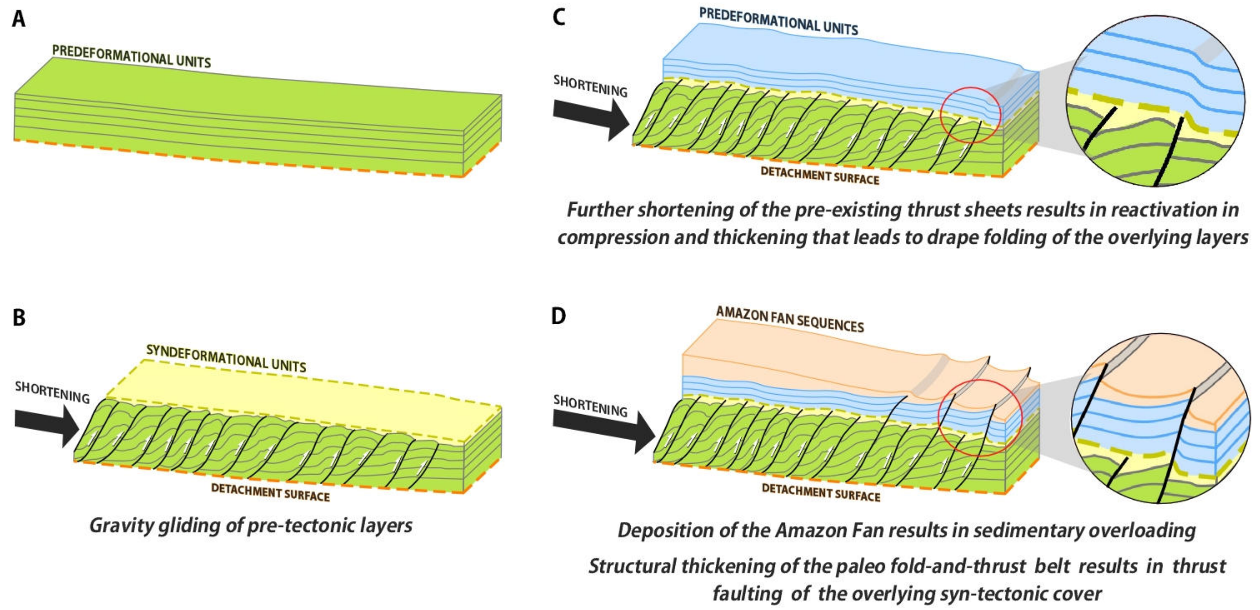


Figure 03 - Simple conceptual models showing possible scenarios for the structural development of fold-and-thrust belts in the geological setting of the Foz do Amazonas basin, relating different degrees of deformation (shortening) to the evolution of the basin's sedimentary infilling, notably the thick clastic wedge of the Amazon Fan. Two gravity-driven deformation mechanisms (Gravity Gliding and Gravity Spreading) were considered (Perovano *et al*., *in preparation*).

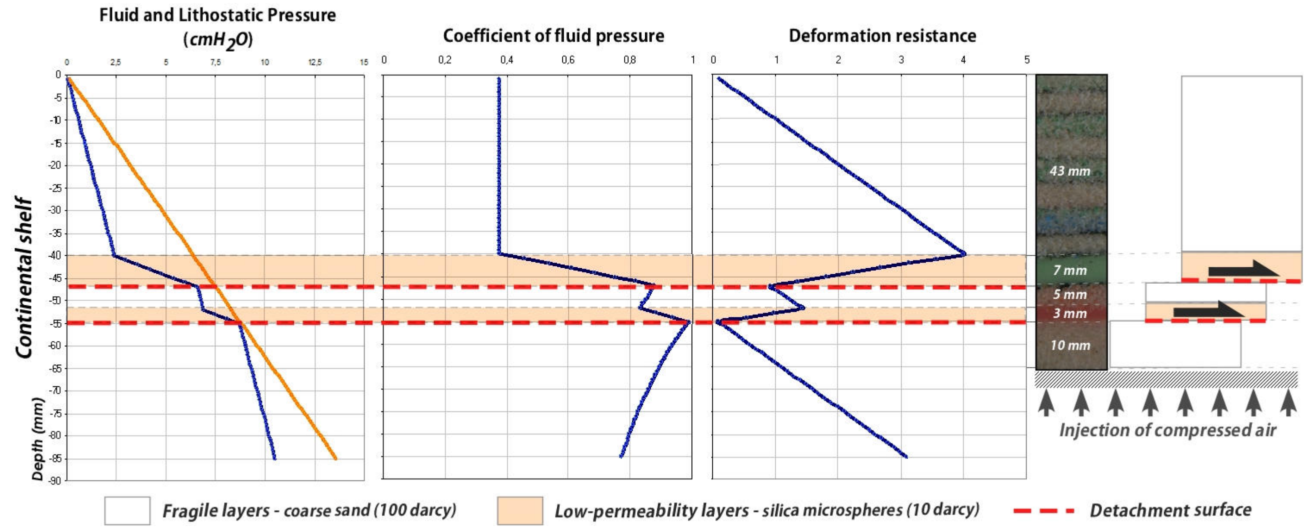


Figure 04 - Numerical simulations of vertical distribution of pressure (fluid and lithostatic), coefficients of fluid pressure and deformation resistance along a multi-layered model having varying permeability. Under pore-fluid overpressure, the levels located at the base of low-permeabillity layers behaved as detachment surfaces, triggering gravitational instabilities. These numerical simulations were previously developed in order to establish each layer's thickness and the fluid pressure magnitude required to induce gravitational instabilities above multiple detachments (Perovano *et al*., *in preparation*).

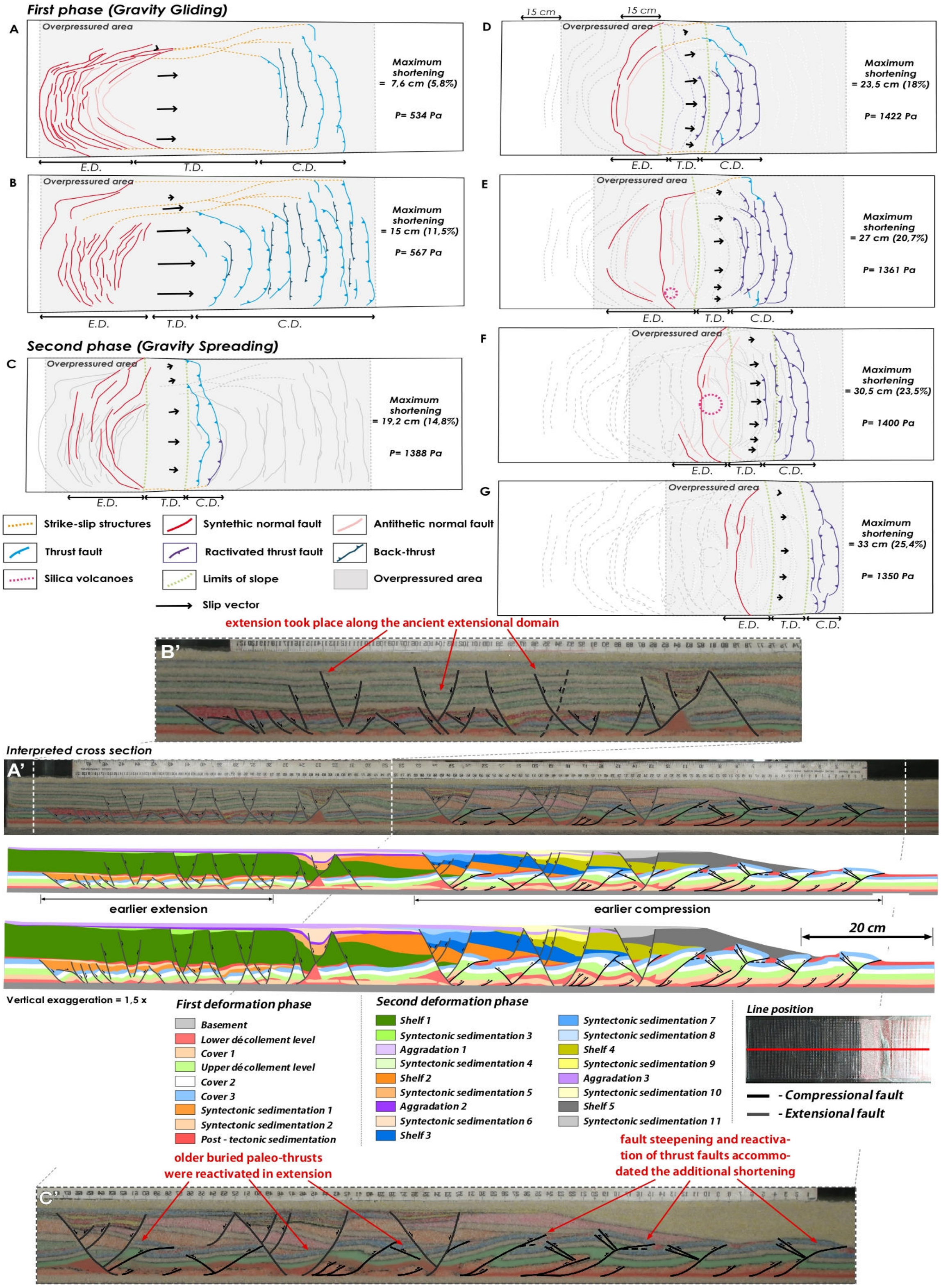


Figure 05 – Interpreted top views of surface structural evolution of the gravitational gliding phase (images A and B) and gravitational spreading phase (images C, D, E, F and G). Dotted lines are inactive structures. The gravity spreading phase simulates the deformation of five progradational sand wedges; (A') Interpreted cross-section of the model 12 illustrating the gravitational structural system that resulted from two main deformation phases. (B') Close up of earlier extensional structures and their reactivation during the second deformation phase. (C') Close up showing the reactivation of older compression structures of the first phase in extension as the sand wedge progradates toward the basin. Distally, the reactivation of ancient compressional structures accommodates additional shortening of the section (Perovano *et al*., *in preparation*).